

Channel Attention Residual U-Net for Retinal Vessel Segmentation

Changlu Guo*, Márton Szemenyei
Department of Control Engineering
and Information Technology
Budapest University of Technology and
Economics
Budapest, Hungary
clguo.ai@gmail.com

Yugen Yi*, Wenle Wang
School of Software
Jiangxi Normal University
Nanchang, Jiangxi
yiygen510@jxnu.edu.cn
wenlewang@jxnu.edu.cn

Wei Zhou
Shenyang Institute of Computing
Technology
Chinese Academy of Science
Shengyang, China
zhouweineu@outlook.com

Abstract—Retinal vessel segmentation is a vital step for the diagnosis of many early eye-related diseases. In this work, we propose a new deep learning model, namely Channel Attention Residual U-Net (CAR-U-Net), to accurately segment retinal vascular and non-vascular pixels. In this model, the channel attention mechanism is introduced into Residual Block and a Channel Attention Residual Block (CARB) is proposed to enhance the discriminative ability of the network by considering the interdependence between the feature channels. Moreover, to prevent the convolutional networks from overfitting, a Structured Dropout Residual Block (SDRB) is proposed, consisting of pre-activation residual block and DropBlock. The results show that our proposed CAR-U-Net has reached the state-of-the-art performance on two publicly available retinal vessel datasets: DRIVE and CHASE DB1.

Keywords—Retinal Vessel Segmentation, CAR-U-Net, channel attention, DropBlock

I. INTRODUCTION

Retinal vessel segmentation is of great significance in the early diagnosis of eye-related diseases. For example, Diabetic Retinopathy (DR) - a universal retinal disease caused by elevated blood sugar - is accompanied by retinal vascular swelling [1]. However, the manual annotation of retinal vessels by ophthalmologists is a slow and labor-intensive task, so researchers have devoted themselves to proposing automatic retinal vessel segmentation methods.

In the past few decades, researchers have proposed a great number of methods for automatic retinal vessel segmentation, which are generally separated into two categories. The first group includes image processing methods, which consist of pre-processing, segmentation, and post-processing steps, such as Bankhead et al. [2], who proposed the use of wavelet transform method to enhance the detection of vessel foreground and background. The other group is made of machine learning-based methods, which mainly use the extracted vector features to train a classifier to classify pixels in the retina. For instance, Lupascu et al. [3] designed 41-D feature vector for every pixel to train the AdaBoost classifier to label each pixel in the retinal image.

Recently, deep learning-based methods have been used for automatic segmentation of retinal vessel and have achieved excellent results. Fu et al. [4] improved the vessel segmentation ability by using a convolutional neural network (CNN) with a Conditional Random Field (CRF) layer and a side output layer. Zhang et al. [5] introduced an edge-based mechanism in U-Net [6] to reach an improved performance. Wu et al. [7] introduced a Multi-Scale Network Followed Network (MS-NFN) for retinal blood vessel segmentation. Although these deep learning-based methods have realized

significant results, the interdependence between the feature channels was ignored. Later, Wang et al. [8] applied channel attention mechanism for skip connection, and channel attention was also successfully applied in other medical image analysis tasks [9, 10]. However, in [8] and [10] only average-pooling is used for aggregating spatial information, but max-pooling collects another important clue about distinctive object features to infer a finer channel-wise attention [16]. Therefore, in this work, we introduce a channel attention mechanism that uses both average-pooled and max-pooled features simultaneously to further improve the performance of retinal vessel segmentation.

In this study, we propose an innovative deep learning-based Channel Attention Residual U-Net (CAR-U-Net) model, which greatly improves the ability of deep neural networks to segment retinal vessels. Specifically, we have the following contributions:

- Inspired by the excellent performance of the residual network [11] and the success of DropBlock in preventing convolutional networks from overfitting [12], we integrate DropBlock into the pre-activation residual block and propose Structured Dropout Residual Block (SDRB). We use the proposed SDRB to build a new deep U-shaped network, which is named Structured Dropout Residual U-Net (SDR-U-Net).
- We consider the relationship between the feature channels, and on the basis of SDRB, we add the channel attention mechanism that uses both average-pooled and max-pooled features simultaneously to propose Channel Attention Residual Block (CARB). Based on these, we propose Channel Attention Residual U-Net (CAR-U-Net).
- We evaluate both models on the DRIVE and CHASE DB1 datasets. The results demonstrate that our proposed CAR-U-Net has surpassed the previous state-of-the-art performance on both datasets.

II. PROPOSED METHOD

A. Network Architecture

The detailed architecture of Channel Attention Residual U-Net (CAR-U-Net) is displayed in Figure 1. The network structure of CAR-U-Net is derived from U-Net, where the original convolution blocks are replaced by the SDRB and CARB. CAR-U-Net contains two paths with the same number of residual blocks, namely the contracting path (left) and the expansive path (right). In the contracting path, each step includes a SDRB, a CARB followed by Batch Normalization (BN), a Rectified Linear Unit (ReLU), and a

2×2 max pooling layer with step size of 2 is used for downsampling. Each step in the expansive path includes using a transposed convolution operation for upsampling, which halves the number of feature channels,

followed by an SDRB, a CARB, BN, and a ReLU. In the last layer, we employ 1×1 convolution and sigmoid activation function to get the required feature map.

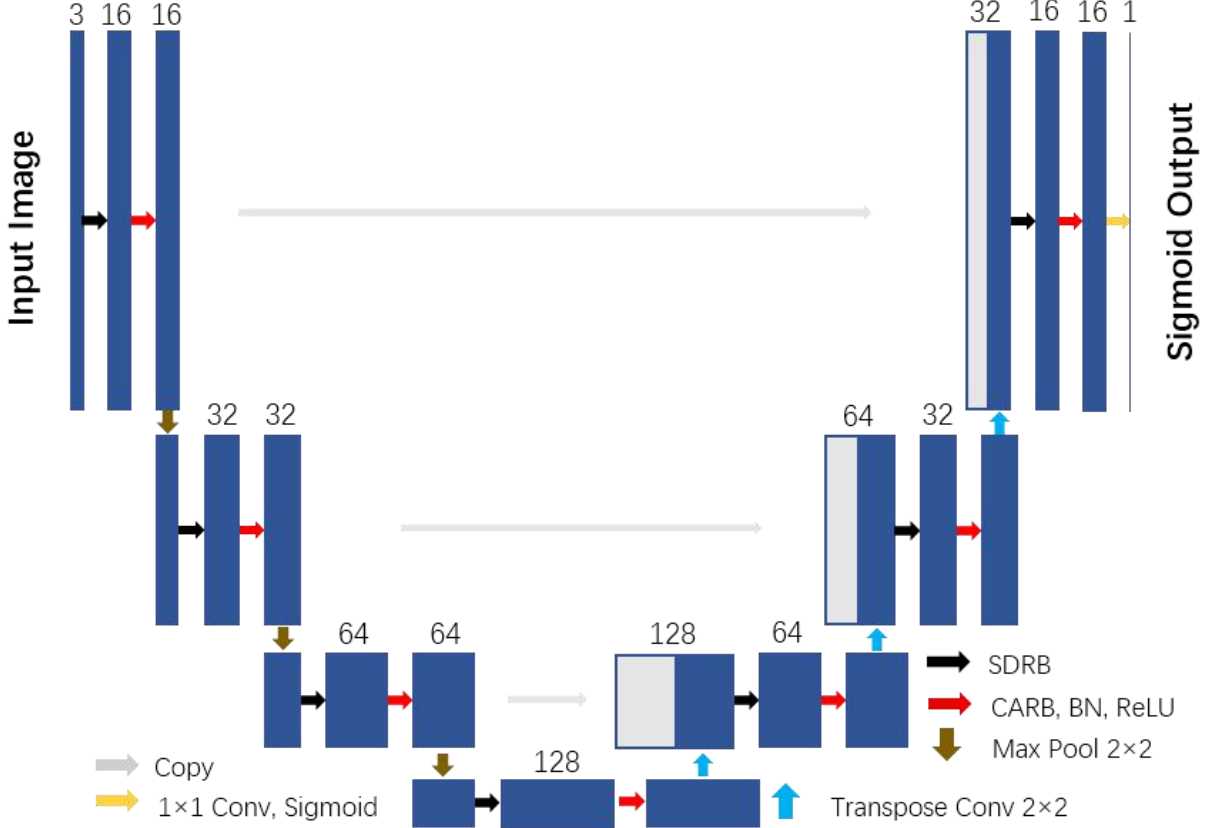


Fig. 1: The CAR-U-Net architecture

B. Channel Attention (CA)

Channel attention was first used as a squeeze and excitation block for classification [15], which generates channel attention maps by using the relationship between the channels, as shown in Fig.2. In order to aggregate the spatial information, we use both average-pooling and maximum-pooling to obtain finer channel-wise attention [16]. Formally, the input feature $F \in R^{H \times W \times C}$ forwarded through the channel-wise max- and average-pooling can generate $F_{mp} \in R^{1 \times 1 \times C}$ and $F_{ap} \in R^{1 \times 1 \times C}$, respectively, e.g., at the c -th channel:

$$F_{mp}^c = \text{Max}(F^c(i, j)), 0 < c < C, 0 < i < H, 0 < j < W \quad (1)$$

$$F_{ap}^c = \frac{1}{H \times W} \sum_{u=1}^H \sum_{j=1}^W F^c(i, j), 0 < c < C \quad (2)$$

where $\text{Max}(\cdot)$ obtains the maximum number, $P^c(\cdot)$ represents the pixel value at a specific position of the c -th channel, and H , W , and C stand for the height, width, and the number of channels of the input feature F , respectively. The two descriptors are then forwarded to a shared weight network consisting of Multi-Layer Perceptron (MLP) with a single hidden layer to generate a channel attention map $M^c \in R^{1 \times 1 \times C}$.

CA sets the hidden activation size to $R^{1 \times 1 \times C/r}$, where r is the reduction rate, which reduces the parameter overhead, and we set the value of r to 16. Then, CA applies the element-wise addition to combine the output feature vectors obtained by the MLP. In short, the channel attention is calculated as:

$$M(F) = \sigma(\text{MLP}(F_{ap}) + \text{MLP}(F_{mp})) \quad (3)$$

where $\text{MLP}(\cdot)$ represents the MLP operation and $\sigma(\cdot)$ denotes the sigmoid function.

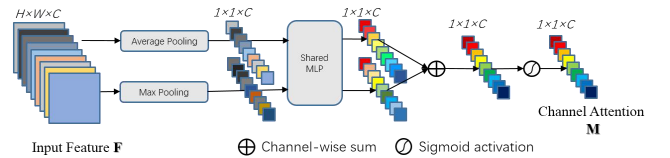


Fig. 2: Diagram of Channel Attention

C. Structured Dropout Residual Block (SDRB)

He et al. [11] observed that when deeper networks begin to converge, there will be a degradation problem: as the network deepens, the accuracy quickly degrades after reaching saturation. In other words, simply deepening the network can hinder training. To overcome these problems, the residual network proposed by He et al. shows

significantly improved training characteristics, allowing the network depth to be previously unachievable. The residual network consists of some stacked residual blocks, and each residual block can be illustrated as a routine form:

$$\begin{aligned} y_i &= F(x_i, w_i) + h(x_i) \\ x_{i+1} &= \sigma(y_i) \end{aligned} \quad (4)$$

where x_i and x_{i+1} represent the input and output of the current residual block, $\sigma(y_i)$ is an activation function, $F(\bullet)$ is the residual function, and $h(x_i)$ is an identity mapping function, typically $h(x_i) = x_i$.

He et al. [13] discussed the effects of diverse combinations in detail and proposed a pre-activation form, as shown in Figure 3 (a). To alleviate the problem of overfitting, we integrate DropBlock [10] into the pre-activation residual block and propose SDRB, as shown in Figure 3 (b). Dropblock is a structured dropout designed specifically for fully convolutional neural networks [14]. In this work, we use this proposed SDRB to build SDR-U-Net. If the number of input and output channels is different, we employ 1×1 convolution to compress or expand the number of channels.

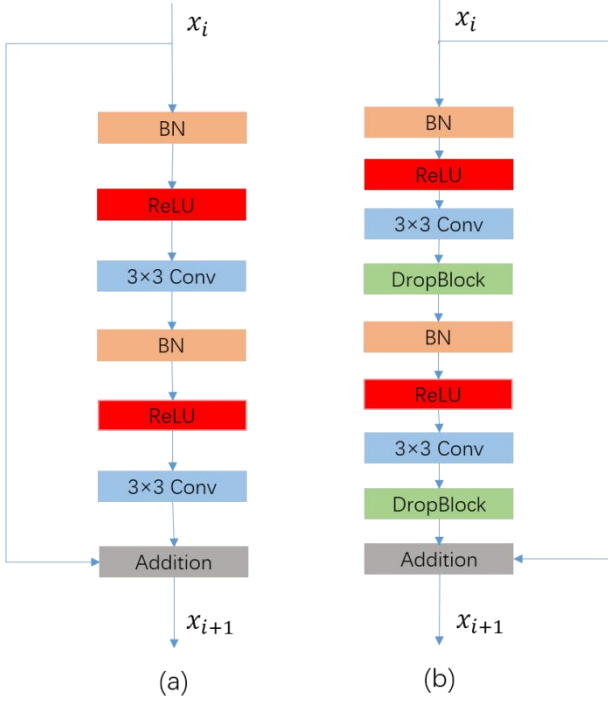


Fig. 3: (a) pre-activation residual block, (b) Proposed Structured Dropout Residual Block

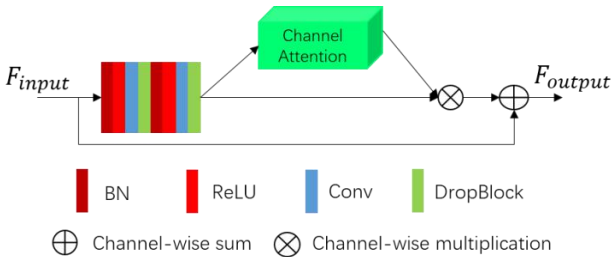


Fig. 4: Diagram of Channel Attention Residual Block

D. Channel Attention Residual Block (CARB)

Channel attention mechanism learns the importance of each feature channel through learning automatically, and uses the obtained importance to enhance features and suppress features that are not important to our retinal vessel segmentation task. In other words, CA can extract channel statistics between channels, thereby further enhancing discriminative ability of the network. Simultaneously, inspired by the success of *squeeze and excitation block* for classification [15], we integrate CA into SDRB and propose CARB, as shown in Figure 4.

III. EXPERIMENTS AND RESULTS

A. Datasets and Preparation

We employ two public retinal fundus image datasets to evaluate our model, they are DRIVE [17] and CHASE DB1 [18]. The DRIVE dataset is collected from a Dutch Diabetic Retinopathy (DR) screening project and contains 40 color fundus images with a resolution of 565×584 pixels. The dataset is partitioned into a training set of 20 images and a testing set of 20 images. CHASE DB1 comes from the British Children's Hearing and Health Research Project, which contains 28 fundus images with a resolution of 999×960 pixels, of which the first 20 images are utilized for training, and the last 8 images are used for testing. The manual annotations of both datasets provided by human experts can be utilized as the ground truth.

To fit our network model, we performed a simple processing on both datasets. We adjusted the size of DRIVE and CHAS DB1 to 592×592 and 1024×1024 by padding it with zero in four margins, respectively. In order to acquire more reasonable results, we crop the segmentation results to the initial size when evaluating.

B. Evaluation Metrics

For the purpose of estimating the performance of the proposed models, the following metrics are employed: Specificity (Spe), Sensitivity (Sen), F1-score ($F1$), Accuracy (Acc), and Area Under the ROC Curve (AUC). Among them, Sen , Spe , Acc and $F1$ can be calculated as follows:

$$Spe = \frac{TN}{TN + FP} \quad (5)$$

$$Sen = \frac{TP}{TP + FN} \quad (6)$$

$$Acc = \frac{TP + TN}{TP + FP + TN + FN} \quad (7)$$

$$F1 = \frac{2TP}{2TP + FN + FP} \quad (8)$$

where TP is true positives, which indicates the blood vessel pixels corresponding to the ground truth are accurately classified into vessels in the segmentation results. If they are misclassified as non-vessels, they are represented as false negatives, namely FN . TN stands for true negatives, which indicates that non-vessel pixels corresponding to the ground truth are accurately classified as non-vessels. If they are inferred to be vessels, they are expressed as false positives, namely FP .

The Area Under the ROC Curve (AUC) can be used to measure the segmentation performance. If the value of AUC is 1, it means flawless segmentation.

TABLE I. RESULTS OF DIFFERENT MODELS ON THE DRIVE AND CHASE DB1 DATASETS (*THE RESULTS ARE OBTAINED FROM [19])

Datasets	DRIVE						CHASE DB1				
Models	Year	<i>Spe</i>	<i>Sen</i>	<i>F1</i>	<i>Acc</i>	<i>AUC</i>	<i>Spe</i>	<i>Sen</i>	<i>F1</i>	<i>Acc</i>	<i>AUC</i>
U-Net[6]*	2015	0.9820	0.7537	0.8142	0.9531	0.9755	0.9701	0.8288	0.7783	0.9578	0.9772
R2U-Net [19]	2018	0.9813	0.7799	0.8171	0.9556	0.9784	0.9820	0.7756	0.7928	0.9634	0.9815
MS-NFN[7]	2018	0.9819	0.7844	-	0.9567	0.9807	0.9847	0.7538	-	0.9637	0.9825
LadderNet [20]	2018	0.9810	0.7856	0.8202	0.9561	0.9793	0.9818	0.7978	0.8031	0.9656	0.9839
DEU-Net[8]	2019	0.9816	0.7940	0.8270	0.9567	0.9772	0.9821	0.8074	0.8037	0.9661	0.9812
Vessel-Net [21]	2019	0.9802	0.8038	-	0.9578	0.9821	0.9814	0.8132	-	0.9661	0.9860
SDR-U-Net	2020	0.9839	0.7953	0.8103	0.9674	0.9828	0.9828	0.8459	0.8050	0.9742	0.9877
CAR-U-Net	2020	0.9847	0.8058	0.8202	0.9691	0.9850	0.9832	0.8435	0.8063	0.9744	0.9884

C. Network Configuration

As mentioned before, we partition the datasets into training and testing sets. In order to further monitor whether our model is overfitting, we randomly select 2 images in the DRIVE and CHASE DB1 training sets respectively as the validation set.

We train this SDR-U-Net and CAR-U-Net from scratch utilizing the training set. For all datasets, we set the number of the feature channels after the first convolutional layer to 16, and utilize the Adam optimizer to optimize our network with binary cross entropy as the loss function. For DRIVE,

the batch size of training is 2, and a total of 200 epochs are trained, of which the first 150 epochs use a learning rate of 1×10^{-3} and the last 50 epochs use 1×10^{-4} . For CHASE DB1, the batch size of training is 1, and a total of 150 epochs are trained, of which the first 100 epochs use a learning rate of 1×10^{-3} and the next 50 epochs use 1×10^{-4} .

For the settings of DropBlock, the size of the discard blocks for all datasets is set to 7, and so as to reach the best performance, we set the dropout rates for DRIVE and CHASE DB1 to 0.14 and 0.22, respectively.

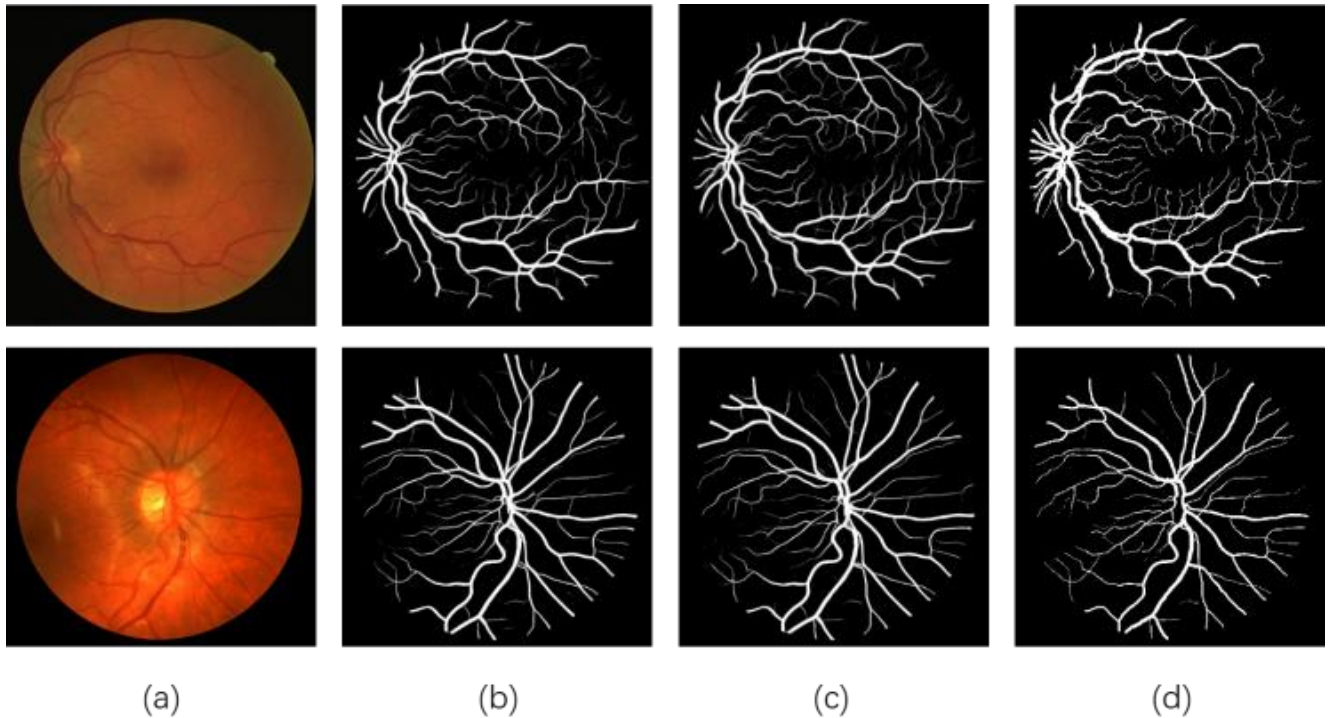


Fig. 5: Row 1 is for DRIVE dataset. Row 2 is for CHASE DB1 dataset. (a) Color fundus images, (b) segmentation results of SDR-U-Ne, (c) segmentation results of CAR-U-Net, (d) corresponding ground truths.

D. Comparison of SDR-U-Net and CAR-U-Net

As mentioned earlier, the only difference between SDR-U-Net and CAR-U-Net is that the latter introduces the channel attention module, so the main content of this section

mainly reflects the impact of the channel attention mechanism on the network.

Examples of the segmentation results of two models are shown in the figures, which are 5 (b) and 5 (c), respectively. For subjective comparison, 5 (d) gives the ground truths for

the fundus images. From the segmentation results, CAR-U-Net achieves better discrimination ability, and can distinguish targets from small blood vessel structures. We also quantitatively compare the performance of the two models in the last two columns of Table 1. We can get the F1, *Acc* and *AUC* on DRIVE and CHASE DB1 of CAR-U-Net are 0.99% / 0.13% , 0.17% / 0.02% and 0.22% / 0.07% respectively higher than SDR-U-Net. These results all prove the effectiveness of the attention strategy of channel attention.

E. Comparisons with the State-of-the-art Models

At last, we compare the proposed CAR-U-Net with several the exiting state-of-the-art models. In Table 1, we sum up the release year of each model and their performance on DRIVE and CHASE DB1 datasets. The results illustrate that, in both datasets, our CAR-U-Net reaches the best performance among all competing models. Specifically, CAR-U-Net has the highest AUC (0.29% / 0.24% higher than the previous best method), the highest accuracy (1.13% / 0.83% higher than the previous best method), the highest sensitivity, and F1-score and specificity are comparable. The above results clearly demonstrate that CAR-U-Net is a competent method for retinal vessel segmentation.

IV. CONCLUSION

In this paper, we presented a Channel Attention Residual U-Net (CAR-U-Net) for retinal vessel segmentation. First, we used the pre-activation residual block with DropBlock to construct SDR-U-Net. In this process, it can not only reduce the degradation problem, but also effectively alleviate the overfitting problem via DropBlock. More importantly, on the basis of SDR-U-Net, CAR-U-Net considers the relationship between the feature channels, so a channel attention mechanism is introduced to strengthen the network's discriminative capability. Our experiments show that CAR-U-Net is significantly superior to the state-of-the-art approaches for retinal vessel segmentation on both DRIVE and CHASE DB1 datasets.

ACKNOWLEDGMENT

This work is supported by the China Scholarship Council, the Stipendium Hungaricum Scholarship, the National Natural Science Foundation of China under Grants 61602221, and Chinese Postdoctoral Science Foundation 2019M661117.

REFERENCES

- [1] I. S. Jacobs and C. P. Bean, Fine particles, thin films and exchange anisotropy, in *Magnetism*, vol. III, G. T. Rado and H. Suhl, Eds. New York: Academic, pp. 271-350, 1963.
- [2] [2]Bankhead, P., Scholfield, C.N., McGeown, J.G., Curtis, T.M.: Fast retinal vessel detection and measurement using wavelets and edge location refinement. *PLoS One* 7(3), e32435 ,2012.
- [3] C. A. Lupascu, D. Tegolo and E. Trucco, "FABC: Retinal Vessel Segmentation Using AdaBoost," in *IEEE Transactions on Information Technology in Biomedicine*, vol. 14, no. 5, pp. 1267-1274, Sept. 2010.
- [4] Fu, H., Xu, Y., Lin, S., Kee Wong, D.W., Liu, J.: DeepVessel: retinal vessel segmentation via deep learning and conditional random field. In: Ourselin, S., Joskowicz, L., Sabuncu, M.R., Unal, G., Wells, W. (eds.) *MICCAI* 2016. LNCS, vol. 9901, pp.132-139. Springer, Cham, 2016.
- [5] Zhang, Y., Chung, A.C.S.: Deep supervision with additional labels for retinal vessel segmentation task. In: Frangi, A.F., Schnabel, J.A., Davatzikos, C., Alberola-López, C., Fichtinger, G. (eds.) *MICCAI* 2018. LNCS, vol. 11071, pp. 83-91. Springer, Cham, 2018.
- [6] Ronneberger, O., Fischer, P., Brox, T.: U-Net: convolutional networks for biomedical image segmentation. In: Navab, N., Hornegger, J., Wells, W.M., Frangi, A.F. (eds.) *MICCAI* 2015. LNCS, vol. 9351, pp. 234-241. Springer, Cham, 2015.
- [7] Wu, Y., Xia, Y., Song, Y., Zhang, Y., Cai, W.: Multiscale network followed network model for retinal vessel segmentation. In: Frangi, A.F., Schnabel, J.A., Davatzikos, C., Alberola-López, C., Fichtinger, G. (eds.) *MICCAI* 2018. LNCS, vol. 11071, pp. 119-126. Springer, Cham, 2018.
- [8] Wang B., Qiu S., He H. (2019) Dual Encoding U-Net for Retinal Vessel Segmentation. In: Shen D. et al. (eds) *MICCAI* 2019. Lecture Notes in Computer Science, vol 11764. Springer, Cham, 2019.
- [9] Mou L. et al. (2019) CS-Net: Channel and Spatial Attention Network for Curvilinear Structure Segmentation. In: Shen D. et al. (eds) *MICCAI* 2019. Lecture Notes in Computer Science, vol 11764. Springer, Cham, 2019.
- [10] Fang Z., Chen Y., Nie D., Lin W., Shen D. (2019) RCA-U-Net: Residual Channel Attention U-Net for Fast Tissue Quantification in Magnetic Resonance Fingerprinting. In: Shen D. et al. (eds) *MICCAI* 2019. Lecture Notes in Computer Science, vol 11766. Springer, Cham, 2019.
- [11] K. He, X. Zhang, S. Ren, and J. Sun, "Deep residual learning for image recognition," in *CVPR*, 2016, pp. 770-778. 2016.
- [12] G. Ghiasi, T.-Y. Lin, and Q. V. Le. DropBlock: A regularization method for convolutional networks. In *Neural Information Processing Systems*, 2018.
- [13] K. He, X. Zhang, S. Ren, and J. Sun. Identity mappings in deep residual networks. In *ECCV*, 2016.
- [14] C. Guo, M. Szemenyei, Y. Pei, Y. Yi and W. Zhou, "SD-Unet: A Structured Dropout U-Net for Retinal Vessel Segmentation," 2019 IEEE 19th International Conference on Bioinformatics and Bioengineering (BIBE), Athens, Greece, 2019, pp. 439-444, 2019.
- [15] J. Hu, L. Shen, and G. Sun. Squeeze-and-excitation networks. In *Proc. IEEE Computer Vision and Pattern Recognition*, pages 7132 - 7141, 2018.
- [16] Sanghyun Woo, Jongchan Park, Joon-Young Lee, and In So Kweon. Cham: Convolutional block attention module. In *The European Conference on Computer Vision (ECCV)*, September 2018.
- [17] J. Staal, M. D. Abramoff, M. Niemeijer, M. A. Viergever, and B. Van Ginneken, Ridge-based vessel segmentation in color images of the retina, *IEEE Transactions on Medical Imaging*, vol. 23, no. 4, pp. 501-509, 2004.
- [18] M. M. Fraz, P. Remagnino, A. Hoppe, et al. An Ensemble Classification-Based Approach Applied to Retinal Blood Vessel Segmentation. *IEEE Transactions on Biomedical Engineering*, 59(9):2538-2548, 2012.
- [19] Alom, M.Z., Hasan, M., Yakopcic, C., Taha, T.M., Asari, V.K.: Recurrent residual convolutional neural network based on u-net (r2u-net) for medical image segmentation. *arXiv preprint arXiv:1802.06955*, 2018.
- [20] Zhuang, J.: Laddernet: multi-path networks based on u-net for medical image segmentation. *arXiv preprint arXiv:1810.07810*, 2018.
- [21] T. Kitrungrotsakul, X.-H. Han, Y. Iwamoto, L. Lin, A. H. Foruzan, W. Xiong, and Y.-W. Chen, "Vesselnets: A deep convolutional neural network with multi pathways for robust hepatic vessel segmentation," *Computerized Medical Imaging and Graphics*, vol. 75, pp. 74 - 83, 2019.